Input Shaped Control of a Gantry Crane with Inertial Payload

Adrian Stein[1] and Tarunraj Singh[2]

***Abstract*— The focus of this work is on the development of a model for a gantry crane transporting a non point-mass payload such as pipes, where besides the payload swinging, includes the twisting motion also, which can be hazardous if not adequately controlled. Euler-Lagrange equations of motion are derived which permit accounting for payloads whose center of mass does not coincide with the hoisting cable attachment. Work-Energy principle is used to ensure that a collocated Proportional-Derivative (PD)-controller is stabilizing and an input shaper is used to shape the reference profile to permit minimal residual vibration of the payload.**

***Index Terms*— Input Shaper, Gantry Crane, Vibration Control.**

I. INTRODUCTION

Dynamic system modeling of cranes has gained increased research interest in recent years with the rise of automation. Transporting heavy payloads has always been challenging, mainly because the payload might undergo large displacements such as swinging or twisting during moving operations. Even with the most experienced crane operators, there are always safety concerns for the crew and the possibility of property damage. There has been a growing interest in the automation of cranes over the past few decades. With companies losing money based on damaged property, inability to operate due to weather conditions, and unskilled crane operators, automation for this process is highly desirable. Fig. 1 shows the outcome of a maneuver by an inexperienced crane operator, creating a potentially catastrophic situation for the operation crew. Zhang et al. [14]

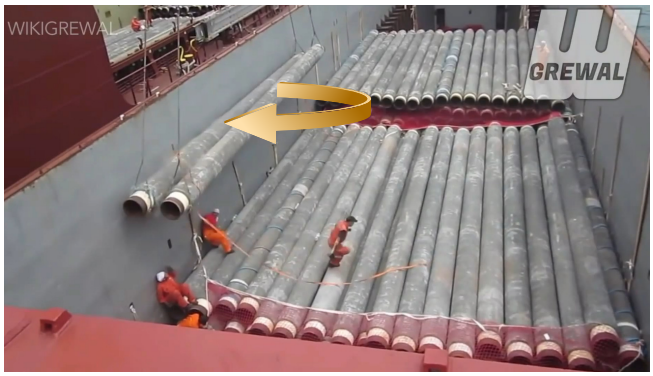

Fig. 1: Twisting payload on a vessel (source:) `https://www.youtube.com/watch?v=DxMG__CD5Qs`).

state that $8\%-16\%$ of all construction fatalities are caused by hoisting-injury accidents. Kim et al. [11] listed 22 out of 40 tower crane accidents in Korea from 2015 to October 2020 were caused by "operation and management" while Raviv et al. [3] categorised 51 accidents and 161 near misses, where "operator error" was ranked 4th with a 13% contribution.

A common choice of controllers for point-to-point maneuvers is a Proportional-Derivative (PD) controller [8]. In order to minimize the oscillations, an open loop approach (input shaping) can be chosen and the main advantage is oscillation suppression without introducing additional sensors to the system. Smith [10] presented the precursor to this method in 1957, after he observed fly fishermen and subsequently developed Input Shaper has been used on various gantry crane models [16]. Compared to open loop control, Sun et al. [6] proposed a super-twisting-based anti-swing control for double pendulum cranes, which is designed to function in a closed loop. Chen et al. [13] also took the bending of the beam into account and how the midspan deflection influences the swinging angle. Giacomelli et al. [18] compared input shaping for double pendulum overhead cranes with input-output inversion control.

The problem with nearly all mathematical models for cranes is that they ignore the inertial properties of the payload [2] [8] [9] [12] [7] [4]. Modelling inertial properties can change the swinging and twisting behavior of the payload. Peng et al. [1] provided a tower crane model where an inertial payload is considered and showed that the twisting motion is initiated by the change in the swinging angles. However, the author isn't aware of any literature which develops gantry crane models with an inertial payload. The additional novelty of this paper is a sensitivity analysis of the swinging and twisting angles with respect to

- uncertain rope length during a moving operation for a hoisted payload
- uncertain center of mass of the payload

when using an input shaped PD-controller for the hoist.

Section II presents a systematic approach to developing a model for the gantry crane with an inertial payload and includes details of the PD controller used in conjunction with an Input Shaper. Section III presents results of the numerical experiments of point-to-point motion control of the gantry crane. The sensitivity of the proposed method to uncertainties in payload's center of mass and rope length are also presented. The paper ends with a concluding section.

II. METHODOLOGY

The task of transporting pipelines can be divided into three maneuvers: lifting, moving and lowering. This applies to both

the unloading and loading on a rig or ship. Fig. 2 shows the desired maneuver of the gantry crane with the payload where (a) illustrates lifting, (b) moving and (c) lowering the payload. Only the moving maneuvers (b) causes twisting of the payload, unless the twist angle is initially not quiescent.

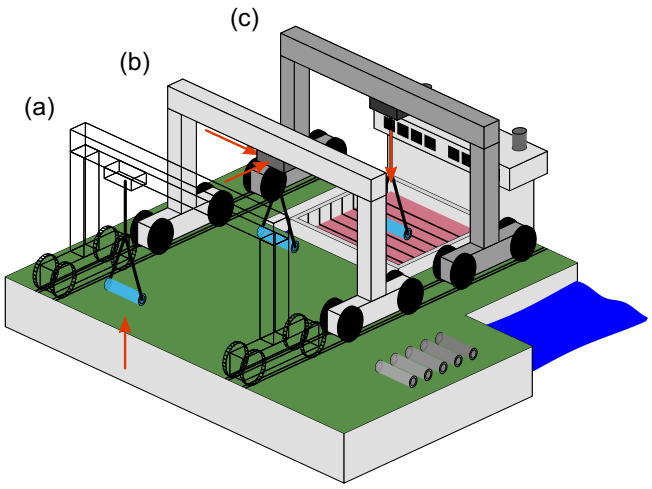

Fig. 2: (a) Lifting the payload. (b) Moving the payload. (c) Lowering the payload.

A. Assumptions

In this paper, the payloads were assumed to be pipelines which are required for offshore oil extraction. An inertial payload was chosen compared to a point mass approach. A hook attached to a rope connects the hoist with the payload. From there, two ropes connect the payload ends with the hook, each of them having the same length and always under tension. Therefore, the ropes can be substituted by a single rope connecting the hoist with the geometrical center of the payload which is always perpendicular to the payload. Furthermore, torsional stiffness for the substituted rope is introduced, while the hook and the rope are assumed to be massless. The crane payload system can be represented as a spherical pendulum and is defined by two swinging angles (δ & ϵ) and one twisting angle (θ). No obstacles are assumed to hinder the payload's movement and no disturbances are considered. The setup is presented in Fig. 3. The values for the gantry crane model are $m_c = 10000$ kg, $m_p = 500$ kg, $r_o = 0.5$ m, $r_i = 0.35$ m, $l_p = 5$ m and $c_t = 1$ Nm/rad, where m_c, m_p, r_o, r_i, l_p, c_t are, respectively, the crane mass (including the hoist), payload mass, outer & inner radius of the payload, length of the payload and the torsional stiffness of the rope. The gravitational constant is set to $g = 9.81 m/s^2$. The initial conditions for the simulation are $x_{init} = 0$ m, $y_{init} = 0$ m, $l_{r,init} = 9.4$ m, $\delta_{init} = 0°$, $\epsilon_{init} = 90°$ and $\theta_{init} = 0°$.

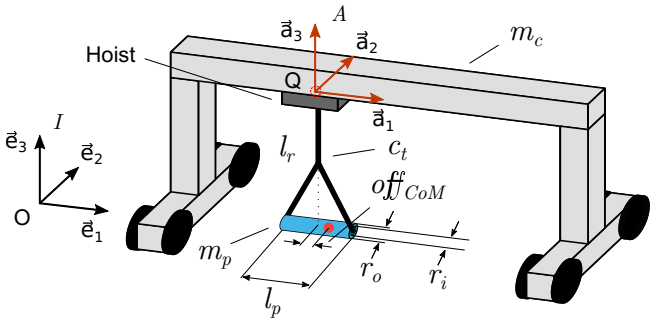

Fig. 3: Gantry crane model with an inertial payload at the initial position ($t = 0s$).

B. Transformation Equations

As a convention, the "right-hand rule" for each reference frame is adopted.

$$\begin{bmatrix}\vec{a}_1\\ \vec{a}_2\\ \vec{a}_3\end{bmatrix} = \begin{bmatrix}1 & 0 & 0\\ 0 & \cos(\delta) & -\sin(\delta)\\ 0 & \sin(\delta) & \cos(\delta)\end{bmatrix}\begin{bmatrix}\vec{b}_1\\ \vec{b}_2\\ \vec{b}_3\end{bmatrix} \quad (1)$$

$$\begin{bmatrix}\vec{b}_1\\ \vec{b}_2\\ \vec{b}_3\end{bmatrix} = \begin{bmatrix}\cos(\epsilon) & 0 & \sin(\epsilon)\\ 0 & 1 & 0\\ -\sin(\epsilon) & 0 & \cos(\epsilon)\end{bmatrix}\begin{bmatrix}\vec{d}_1\\ \vec{d}_2\\ \vec{d}_3\end{bmatrix} \quad (2)$$

$$\begin{bmatrix}\vec{d}_1\\ \vec{d}_2\\ \vec{d}_3\end{bmatrix} = \begin{bmatrix}1 & 0 & 0\\ 0 & \cos(\theta) & -\sin(\theta)\\ 0 & \sin(\theta) & \cos(\theta)\end{bmatrix}\begin{bmatrix}\vec{f}_1\\ \vec{f}_2\\ \vec{f}_3\end{bmatrix} \quad (3)$$

Eq. (1), (2) and (3) represent the transformation equations with respect to the swinging angles δ and ϵ and the twisting angle θ. Fig. 4 illustrates the transformation equations applied on the gantry crane model.

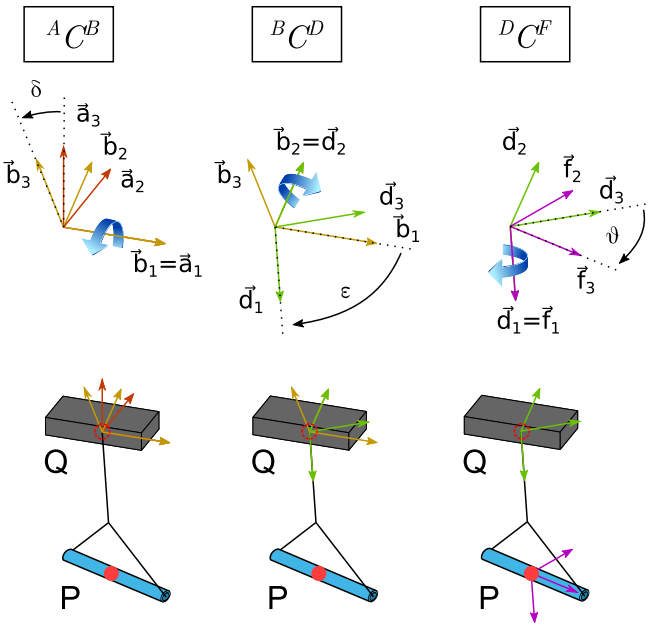

Fig. 4: Transformation of the reference frames $^{A}C^{B}$, $^{B}C^{D}$ and $^{D}C^{F}$.

C. Kinematics

For the default case, the payload's center of mass (CoM) is in the middle of the payload, so the payload's mass is assumed to be uniformly distributed. The vector, which points at the CoM can be described as

$$\begin{aligned} {}^{I}\mathbf{r}_{P,O} &= x\vec{e}_1 + y\vec{e}_2 + l_r\vec{f}_1 ... \\ &= x\vec{e}_1 + y\vec{e}_2 + l_r\vec{d}_1 = x\vec{e}_1 + y\vec{e}_2 ... \\ ... + l_r\left(\cos(\epsilon)\vec{b}_1 - \sin(\epsilon)\vec{b}_3\right) &= x\vec{e}_1 + y\vec{e}_2 ... \\ ... + l_r\cos(\epsilon)\vec{e}_1 - l_r\sin(\epsilon)\left(-\sin(\delta)\vec{e}_2 + \cos(\delta)\vec{e}_3\right) & \quad (4) \\ \rightarrow {}^{I}\mathbf{v}_{P,O} = {}^{I}\frac{d}{dt}({}^{I}\mathbf{r}_{P,O}) & \quad (5) \end{aligned}$$

where Eq. (5) describes the velocity. Motors move the hoist in $\vec{e}_1$ and $\vec{e}_2$ direction, while the displacement in $\vec{e}_1$ is denoted with x and in $\vec{e}_2$ with y. A winch controls the rope length l_r. These variables are the only ones being controlled, making the system underactuated.

D. Moment of Inertia Matrices

The angular velocities can be written as follows:

$$\left[{}^{I}\boldsymbol{\omega}^{B}\right]_I = \left[{}^{A}\boldsymbol{\omega}^{B}\right]_A = \left[{}^{A}\boldsymbol{\omega}^{B}\right]_B = \dot{\delta}\ \vec{a_1} = \dot{\delta}\ \vec{b_1} \quad (6)$$

$$\left[{}^{B}\boldsymbol{\omega}^{D}\right]_B = \left[{}^{B}\boldsymbol{\omega}^{D}\right]_D = \dot{\epsilon}\ \vec{b_2} = \dot{\epsilon}\ \vec{d_2} \quad (7)$$

$$\left[{}^{D}\boldsymbol{\omega}^{F}\right]_D = \left[{}^{D}\boldsymbol{\omega}^{F}\right]_F = \dot{\theta}\ \vec{d_1} = \dot{\theta}\ \vec{f_1} \quad (8)$$

The inertia matrix for the payload is

$$\left[\mathbf{I}_{p,CoM}\right]_F = \begin{pmatrix} I_{1,2} & 0 & 0 \\ 0 & I_{1,2} & 0 \\ 0 & 0 & I_3 \end{pmatrix} \quad (9)$$

where $I_{1,2}$ is representing the moment of inertia about the $\vec{f_1}$ and $\vec{f_2}$ axes, and I_3 for the $\vec{f_3}$ axis with respect to the CoM. The moment of inertias can be calculated as

$$I_{1,2} = \frac{m_p}{12}\left(3\left(r_o^2 + r_i^2\right) + l_p^2\right) \quad (10)$$

$$I_3 = \frac{m_p}{2}\left(r_o^2 + r_i^2\right) \quad (11)$$

which is the equation of a hollow cylinder [15]. Any offset of the CoM needs to be modelled with the parallel axis theorem. Kasdin and Paley [17] defined the rotational part of the kinetic energy as

$$T_{p,rot} = \frac{1}{2}\left[{}^{I}\boldsymbol{\omega}^{F}\right]_F^T\left[\mathbf{I}_{p,CoM}\right]_F\left[{}^{I}\boldsymbol{\omega}^{F}\right]_F \quad (12)$$

$$\begin{aligned} \left[{}^{I}\boldsymbol{\omega}^{F}\right]_F = \Big[& \left({}^{B}C^{D}\ {}^{D}C^{F}\right)^T\left[{}^{I}\boldsymbol{\omega}^{B}\right]_B + ... \\ & ...\left({}^{D}C^{F}\right)^T\left[{}^{B}\boldsymbol{\omega}^{D}\right]_D + \left[{}^{D}\boldsymbol{\omega}^{F}\right]_F\Big]_F \end{aligned} \quad (13)$$

E. Energy

In order to apply the Lagrangian approach, the kinetic and potential energy of the system needs to be calculated. Using the notation of [17], the kinetic and potential energy can be written as

$$\begin{aligned} T_O = & \frac{m_c}{2}||{}^{I}\mathbf{v}_{Q,O}||^2 + \frac{m_p}{2}||{}^{I}\mathbf{v}_{P,O}||^2 + ... \\ & ...\frac{1}{2}\left[{}^{I}\boldsymbol{\omega}^{F}\right]_F^T\left[\mathbf{I}_{p,CoM}\right]_F\left[{}^{I}\boldsymbol{\omega}^{F}\right]_F \quad (14) \end{aligned}$$

$$U_O = m_c g h + m_p g\left(h - l_r\right) + \frac{1}{2}c_t\theta^2 \quad (15)$$

In order to perform operations like lifting and lowering the payload onto a vessel, the zero potential energy level is modelled with some constant height h (here $h = 20$ m), which needs to be greater than $max(l_r)$.

F. Lagrangian

Kasdin and Paley [17] defined the Lagrangian and Euler-Lagrangian approach as

$$L_O = T_O - U_O \quad (16)$$

$$\frac{{}^{I}d}{dt}\left(\frac{\partial L_O}{\partial \dot{q}_j}\right) - \frac{\partial L_O}{\partial q_j} = \tau_j \quad (17)$$

where τ_j are the non-conservative applied forces and q_j are the generalized coordinates. Any constant term in the energy formulation won't affect the states.

G. Control Methods

The scope of the control problem is rapid point-to-point motion of a payload with the goal of minimizing the residual energy at the end of the maneuver. This includes the swinging and twisting motion of the payload. Fig. 5 is a time-lapse illustration of the input shaped motion control of a gantry crane highlighting the motion of a simple pendulum when a point-to-point maneuver is required. The PD-controller

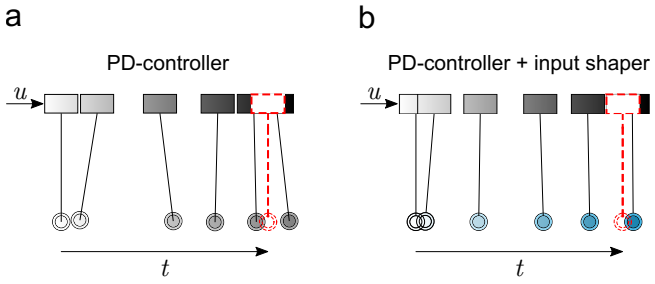

Fig. 5: (a) Proportional-Derivative controller, and (b) Input shaped Proportional-Derivative controller on a simple pendulum for a point-to-point maneuver over time, where the dashed red pendulum is the desired position and u is the input.

causes large oscillations in the system, while the PD-controller used in conjunction with an input shaper results in a response with significantly smaller oscillations. The control law for the present gantry crane model in this paper is

$$\tau_x = k_p\left(x_{ref} - x\right) + k_d\left(0 - v_x\right) \quad (18)$$

$$\tau_y = k_p\left(y_{ref} - y\right) + k_d\left(0 - v_y\right) \quad (19)$$

$$\tau_{l_r} = 5k_p\left(l_{r,ref} - l_r\right) + 0.5k_d\left(0 - v_{l_r}\right) \quad (20)$$

where $k_p = 1250$ and $k_d = 5000$ are the P- and D-gains. The system is modelled with six degrees of freedom, but only three are actuated. The main focus of this paper is to show the benefit of input shaping during the "move" maneuver, so the controller gains are not tuned. Fig. 6 illustrates the block diagram and the functionality of an input shaper where the main goal is to minimize the oscillations of the plant/system. Due to the high nonlinearity of the system, linearization can

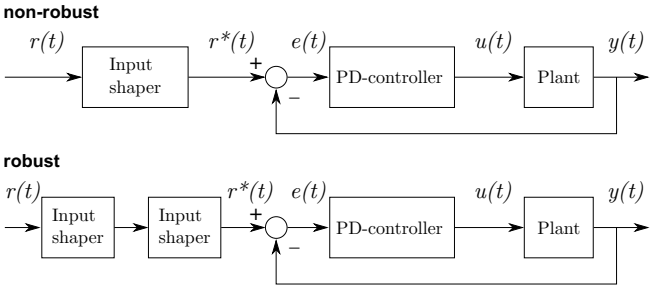

Fig. 6: Block diagram of an non-robust/robust input shaped PD-controller (robust: here two cascaded input shapers).

lead to poor results based on the operating point about which the model is linearized. In this paper, the natural frequency (ω_n) is determined with a fast fourier transformation of a typical response of the crane model to a step input. Later, the rope length l_r and the CoM (with off_{CoM}) will be changed in order to complete a sensitivity analysis for a non-robust versus a robust case.

H. System Identification and Input Shaping

For designing the input shaper it is assumed that $off_{CoM} = 0$ m, hence the natural frequency is only influenced by the rope length $l_{r,move}$. Therefore, the "lifted" part of the operation is of concern. The natural frequency is determined by applying a reference profile on y as it is shown in Fig. 7, while x is uncontrolled. For this part, the P- and D-

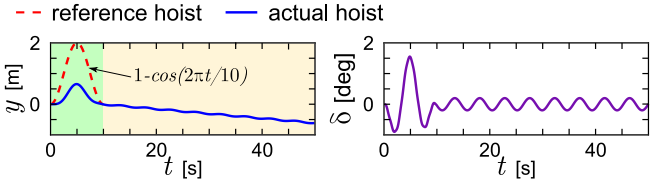

Fig. 7: Approach to determine the natural frequency for the lifted payload.

gain for y are scaled up by the factor of 100. The controller is acting for $0-10$ s and is then turned off in order to let the system oscillate. The fast fourier transformation shows that the dominant frequency of angle δ is $f = 0.22$ Hz, which is equal to $\omega_n = 0.44\pi$ rad/s. Singh [5] defined a time-delay filter as an input shaper as

$$G_{nonrob}(s) = A_0 + A_1 exp(-sT) \quad (21)$$

$$\rightarrow A_0 + A_1 exp(-sT) = 0 \quad (22)$$

where

$$A_0 = \frac{exp\left(\frac{\zeta\pi}{\sqrt{1-\zeta^2}}\right)}{1 + exp\left(\frac{\zeta\pi}{\sqrt{1-\zeta^2}}\right)} \approx 0.5079 \quad (23)$$

$$A_1 = 1 - A_0 = 0.4921 \quad (24)$$

$$T = \frac{\pi}{\omega_0\sqrt{1-\zeta^2}} = 2.2728s \quad (25)$$

where A_0 is the magnitude of the proportional signal and T is the delay time. ζ is assumed to be 0.01. The complete input shaper is:

$$G_{nonrob}(s) = 0.5079 + 0.4921 exp(-2.2728s) = 0 \quad (26)$$

and the robust input shaper is selected to place two sets of zeros at the nominal location of the underdamped poles of the system resulting in the shaper:

$$G_{rob}(s) = (A_0 + A_1 exp(-sT))^2. \quad (27)$$

The two delay input-shaper was selected to account for the uncertainties in the rope length, inertial payload offset and the nonlinearity of the dynamic system. Another option to deal with uncertainties is a minimax filter which has the following structure [19]:

$$G_{minimax}(s) = A_0 + A_1 exp(-sT_1) + A_2 exp(-sT_2) \quad (28)$$

$$A_0 = \frac{2\left(1 + \cos\left(\frac{\omega_L\pi}{\omega}\right)\right)}{5 + 4\cos\left(\frac{\omega_L\pi}{\omega}\right) - \cos\left(\frac{2\omega_L\pi}{\omega}\right)} \quad (29)$$

$$A_1 = 1 - 2A_0 \quad (30)$$

$$A_2 = A_0 \quad (31)$$

$$T_1 = \frac{\pi}{\omega} \quad (32)$$

$$T_2 = 2T_1 \quad (33)$$

where $\omega = (\omega_U + \omega_L)/2$ with $\omega_L = 0.2794$ rad/s and $\omega_U = 0.519$ rad/s.

III. RESULTS

The operation of the gantry crane with the inertial payload is divided into three sub-operations, previously presented in Fig. 2. The following times were chosen for each sub-operation: lifting: $0-10$ s, moving: $10-40$ s and lowering: $40-50$ s. Fig. 8 shows the evolution of the states x, y and l_r for the whole operation. Since no integral gain was included for any of the controllers, a steady-state error applied to the controlled states. This was most obvious for the state l_r. Fig. 9(a) shows that the PD-controller created large oscillations in the swinging angles δ and ϵ. Furthermore, a large twist was observed. The input shaped PD-controller created a response with significantly smaller oscillations. As an evaluation tool, one could choose the difference between the maximum and the minimum angle value for each angular displacement, furthermore denoted as Δ. Swinging angle δ and ϵ were reduced about 65.9% and 63.2% respectively,

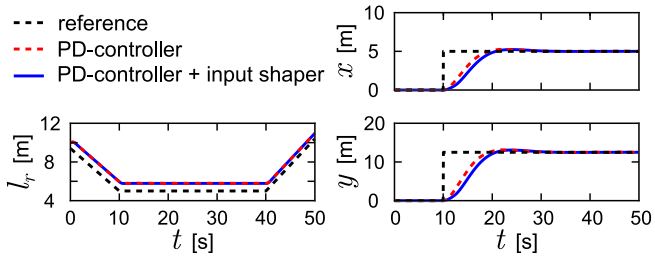

Fig. 8: Evolution of the the states x, y and l_r during the operation.

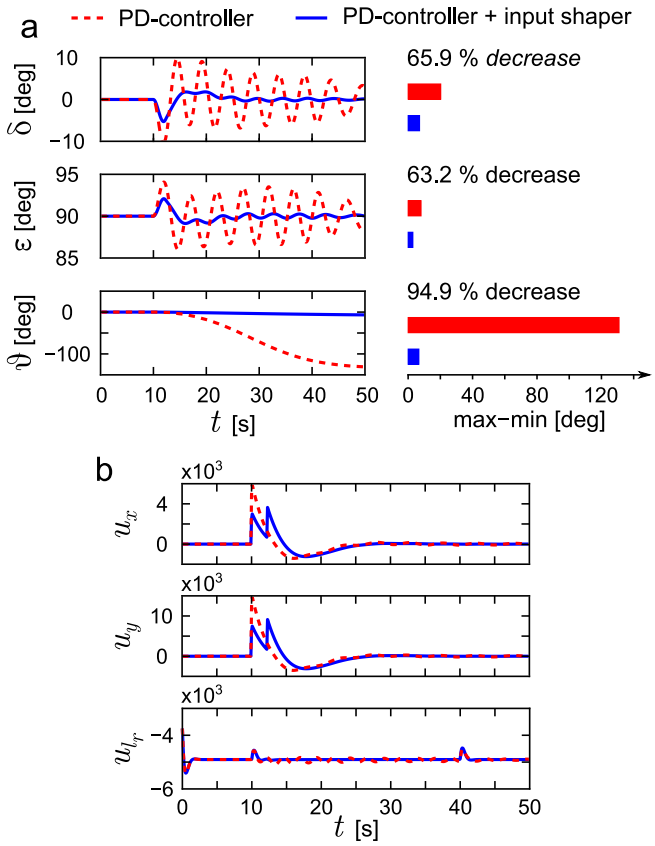

Fig. 9: (a) Evolution of the swinging angles δ & ϵ and the twisting angle θ during the operation. (b) Input on x, y and l_r during the operation.

while θ decreased about 94.9%. Fig. 9(b) shows that the input shaper reduced the acceleration in x and y at $t = 10$ s by splitting the control input into two. The control u_{l_r} showed small oscillations for the normal PD-controller because it had to compensate for the displacements caused by the swinging payload.

A. Non-Robust vs Robust vs Minimax

The input shaper was set up for a rope length $l_{r,move} = 5$ m, but this cannot always be guaranteed. For instance, if an object needs to be avoided, $l_{r,move}$ could change and a perturbation needs to incorporated. Furthermore, a non-uniformly distributed mass of the payload could cause the CoM to be displaced from the geometrical center of the payload, which is addressed by off_{CoM} (see Fig. 3). A change in the x and y trajectories due to perturbations in $l_{r,move}$ and the CoM of the payload is negligible and makes each configuration comparable. Fig. 10 shows the difference between the maximum and the minimum angle value of each angle respectively, when $l_{r,move}$ and off_{CoM} are perturbed. The robust input shaped PD-controller outperforms the non-robust design for any considered perturbation. For the angle ϵ just a small improvement can be noted but a greater one was observed in δ because the main movement happens in $\vec{e}_2$ direction (from 0 m to 12.5 m). For the design point ($l_{r,move} = 5$ m and $off_{CoM} = 0$ m) it resulted in respective reductions of δ, ϵ and θ by 77.1%, 76.7% and 98.3%, when compared to a PD-controller. Fig. 11 shows the improvement

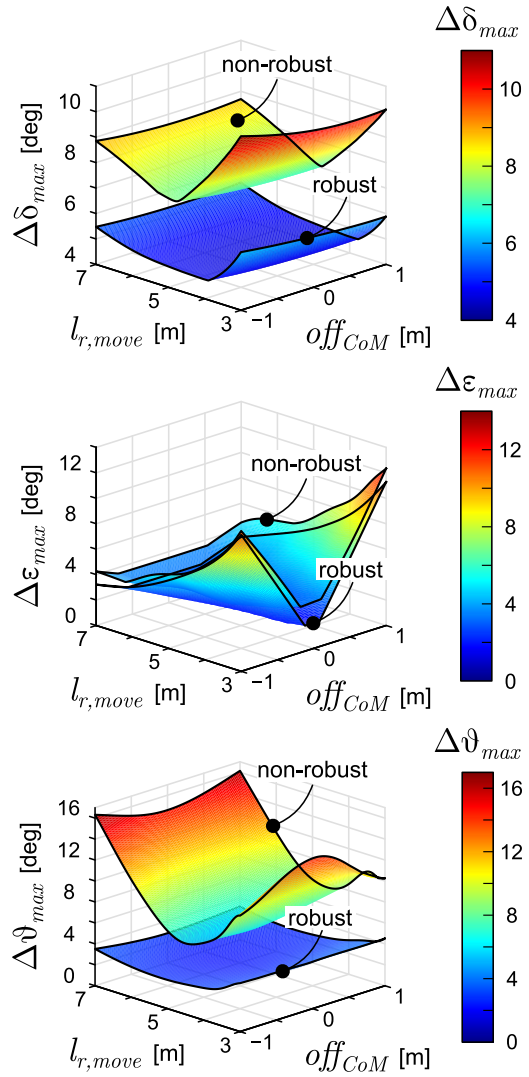

Fig. 10: Difference between the maximum and minimum angle value of the swinging angles $\Delta\delta_{max}$ & $\Delta\epsilon_{max}$ and the twisting angle $\Delta\theta_{max}$ of a robust design compared to a non-robust filter when the payload's center of mass and the rope length are perturbed.

of using a minimax filter instead of a robust solution on the

difference between the maximum and the minimum angle value of each angle respectively, when $l_{r,move}$ and off_{CoM} are perturbed. For all three angles it can be seen that the minimax design is outperforming the robust filter for extreme perturbation cases e.g. $l_{r,move} = 7$ m and $off_{CoM} = 1$ m. No improvement was observed around the design point ($l_{r,move} = 5$ m and $off_{CoM} = 0$ m), which matches the nature of a minimax design.

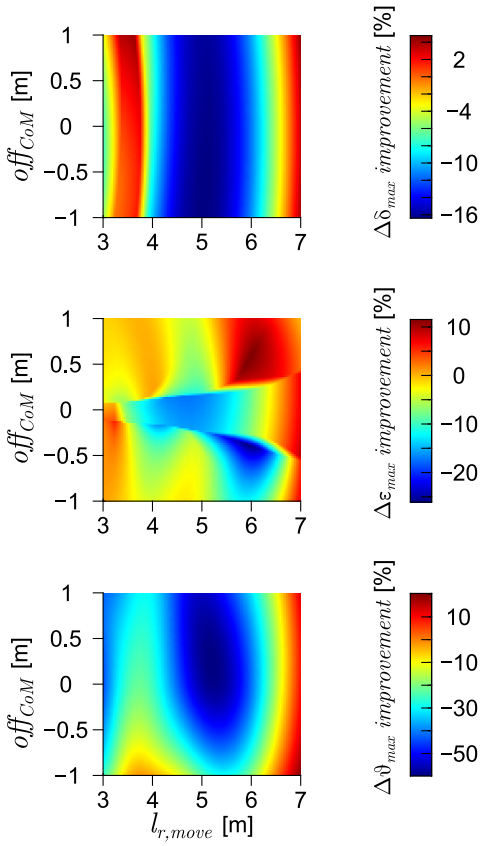

Fig. 11: Improvement on the difference between the maximum and minimum angle value of the swinging angles $\Delta\delta_{max}$ & $\Delta\epsilon_{max}$ and the twisting angle $\Delta\theta_{max}$ of a minimax filter compared to a robust filter when the payload's center of mass and the rope length are perturbed.

IV. CONCLUSIONS

There are many instances where mistakes by gantry crane operators have caused large damage to property and endangered operating crews. In this paper, a gantry crane model with an inertial payload was studied where the payload was modelled as a pipeline. An application of input shaping to the PD-controller of the hoist reduced the swinging and twisting of the payload tremendously compared to a standard PD-controller. Furthermore, a sensitivity analysis with respect to the rope length and the payload's center of mass showed the advantage of robust input shaping. It can be shown that for extreme perturbation cases it might be appropriate to use a minimax filter. An experimental setup is currently under construction for validating the twist-control of inertial payloads for point-to-point maneuvers.

REFERENCES

[1] Peng, J., Huang, J., & Singhose, W. (2019). Payload twisting dynamics and oscillation suppression of tower cranes during slewing motions. Nonlinear Dynamics, 98(2), 1041–1048.

[2] Poljak, D., Schindele, D., Antritter, F., Aschemann, H., & Hillermeier, C. (2010). Control of an Overhead Crane with the Controlled Lagrangian Method. IFAC Proceedings Volumes, 43(14), 131–136.

[3] Raviv, G., Fishbain, B., & Shapira, A. (2017). Analyzing risk factors in crane-related near-miss and accident reports. Safety Science, 91(4), 192–205.

[4] Shi, H., Li, G., Ma, X., & Sun, J. (2019). Research on Nonlinear Coupling Anti-Swing Control Method of Double Pendulum Gantry Crane Based on Improved Energy. Symmetry, 11(12), 1511.

[5] Singh, T. (2010). Optimal reference shaping for dynamical systems: Theory and applications / Tarunraj Singh. CRC Press.

[6] Sun, N., Fang, Y., Chen, H., & Fu, Y. (2015). Super-twisting-based antiswing control for underactuated double pendulum cranes. In 2015 IEEE International Conference on Advanced Intelligent Mechatronics (AIM) (pp. 749–754). IEEE.

[7] Vázquez, C., Collado, J., & Fridman, L. (2014). Super twisting control of a parametrically excited overhead crane. Journal of the Franklin Institute, 351(4), 2283–2298.

[8] Zawawi, M., Bidin, J., Tumari, M., & Saealal, M. (2011). Investigation of Classical and Fuzzy Controller Robustness for Gantry Crane System Incorporating Payload. In 2011 Third International Conference on Computational Intelligence, Modelling & Simulation (pp. 141–146). IEEE.

[9] Zawawi, M., Zamani, W., Ahmad, M., Saealal, M., & Samin, R. (2011). Feedback control schemes for gantry crane system incorporating payload. In 2011 IEEE Symposium on Industrial Electronics and Applications (pp. 370–375). IEEE.

[10] M. Smith, O. (1957). Posicast Control of Damped Oscillatory Systems. Proceedings of the IRE, 45(9), 1249–1255.

[11] Kim, J., Lee, D., Kim, J., & Kim, G. (2021). Priority of Accident Cause Based on Tower Crane Type for the Realization of Sustainable Management at Korean Construction Sites. Sustainability, 13(1), 242.

[12] Cai, T., Zhang, H., Gu, L., & Gao, Z. (2013). On active disturbance rejection control of the payload position for gantry cranes. In 2013 American Control Conference (pp. 425–430). IEEE.

[13] Chen, Q., Cheng, W., Gao, L., & Du, R. (2020). Dynamic Response of a Gantry Crane's Beam Subjected to a Two-Axle Moving Trolley. Mathematical Problems in Engineering, 2020(1), 1–10.

[14] Zhang, W., Zhu, S., Zhang, X., & Zhao, T. (2020). Identification of critical causes of construction accidents in China using a model based on system thinking and case analysis. Safety Science, 121(1), 606–618.

[15] Grote, K.-H and Feldhusen, J. (2014). Dubbel: Taschenbuch für den Maschinenbau : mit mehr als 3000 Abbildungen und Tabellen. Springer Berlin.

[16] Huang, J., Xie, X., & Liang, Z. (2015). Control of Bridge Cranes With Distributed-Mass Payload Dynamics. IEEE/ASME Transactions on Mechatronics, 20(1), 481–486.

[17] Kasdin, N., & Paley, D. (2011). Engineering dynamics: A comprehensive introduction / N. Jeremy Kasdin & Derek A. Paley. Princeton University Press.

[18] Giacomelli, M., Padula, F., Simoni, L., & Visioli, A. (2018). Simplified input-output inversion control of a double pendulum overhead crane for residual oscillations reduction. Mechatronics, 56(7), 37–47.

[19] Singh, T. and Muenchhof, M. 2007, Closed-form minimax time-delay filters for underdamped systems. Optimal Control Applications and Methods 28(3),